PERMEABILITY CHARACTERIZATION ON TIGHT GAS SAMPLES USING PORE PRESSURE OSCILLATION METHOD

Y. Wang and R. J. Knabe
Shell International E & P, Inc., Houston, USA

This paper was prepared for presentation at the International Symposium of the Society of Core Analysts held in Halifax, Nova Scotia, Canada, 4-7 October, 2010

ABSTRACT

For unconventional gas reservoirs, permeability, an important parameter in the subsurface evaluation, is typically low ($\leq 10^{-3}$ mD). While several approaches have been proposed and used, determination of permeability of microdarcy or lower still remains challenging. In a pore pressure oscillation method, the sample is first stabilized at certain pore pressure, then a small sinusoidal pressure wave is applied to the upstream side of the sample, and the pressure response at the downstream side is recorded. Permeability is deduced from the attenuation and phase shift of the downstream signal. When compared with other methods, this technique greatly reduces the pore pressure variation, increases the measurement sensitivity, and results in more accurate characterization. We have applied this technique in permeability characterization for various reservoirs. The results provided valuable input in subsurface modeling and production forecasting.

INTRODUCTION

As the energy demand increases, technology and geological knowledge advance, production from unconventional gas formations, such as tight gas sands, is beginning to make up larger percentage in the supply. Tight gas sand has very low permeability ($\leq 10^{-3}$ mD) and is often inter-bedded with shale. Therefore communication between sand pockets is poor, and numerous wells may be required to access the reservoir. Indeed, two of the most difficult parameters to evaluate in tight gas reservoirs are size and shape of drainage-area. For such tight formations, permeability is of fundamental importance for adequate reservoir characterization. It is an important parameter in evaluation of drainage-area, optimization of well number and location, as well as the drilling and completion procedures.

In the history of core analysis, several approaches to measure low permeability have been developed. Those methods are typically split into two main categories: steady state (SS) method and unsteady state (USS) method. In a SS method, either constant pressure head or constant fluid flow is applied, and permeability is calculated directly from the Darcy's Law. Traditional SS method to measure low permeability samples involves imposing significant pressure difference between the upstream and downstream of the sample. The difference in pore pressure causes unwanted stress variations on the sample. Besides, it

takes time to establish steady flow in a SS measurement. For tight samples, the time can be days or even weeks. On the other hand, in a USS method, a pressure pulse is applied at the upstream end of rock sample. Downstream end of the sample is either connected to a reservoir or open to the air. Permeability is deduced from the pressure transient response [1-4]. It greatly reduces the experiment duration. However, for very low permeability samples, measured pressure is very sensitive to the temperature variation and other noise. As a result, data interpretation from USS method can be complicated and noise sensitive. Moreover, microscopic heterogeneity may potentially dominate the measured pressure decay.

The pore pressure oscillation technique can be considered as a hybrid method of SS and USS measurements. It was originally suggested in the 90's as an extension of a method for measuring hydraulic diffusivity [5]. Fischer discussed the theoretical background, design considerations in experiments, and data analysis comprehensively in Ref. [6]. Bernabé *et. al.* used a different set of dimensionless parameters to solve for permeability and sample storage capacity, and analyzed their uncertainties in details [7]. The method has been used in permeability characterization for different materials [8, 9]. It was also extended by Boitnott [10] to measure the rock sample with high permeability, using complex pore pressure transients. To our knowledge, little work has been done to apply this method in unconventional gas samples with very low permeabilities. On the other hand, measuring very low permeability sample still remains challenging. It is the objective of this work to characterize the permeability for tight gas samples using pore pressure oscillation method. We will briefly discuss the theoretical background of this method, present our results, and discuss its advantages, uncertainties and possible applications.

THEORETICAL BACKGROUND

In a pore pressure oscillation method, the sample is first stabilized at certain pore pressure P_0, then a small sinusoidal pressure oscillation is applied to the upstream side of the sample, and the pressure response at the downstream side is recorded. Permeability is deduced from the amplitude attenuation and phase shift of the downstream signal. Detailed discussion on the theory of the pore pressure oscillation technique can be found in Ref. [6, 7].

General flow equation for slightly compressible fluid in one dimensional porous media is

$$\frac{\partial^2 P}{\partial x^2} = \frac{\mu \beta_s}{k} \frac{\partial P}{\partial t} , \qquad (1)$$

where P is pressure, k is permeability of the sample, μ is fluid viscosity, and β_s is storage capacity of the sample – fluid system. It is noted that the more rigorous treatment for gas flow in porous media is a nonlinear equation. In the derivation of analytical solutions, we have used the above linear equation and its validity will be discussed later.
Eq. (1) is a one–dimension diffusion–like equation and can be solved for certain initial and boundary conditions. For the pore pressure oscillation method, those conditions are

$$P(x,0) = 0 , \qquad (2)$$

$$P_d(0) = 0, \quad \left(\frac{\partial P}{\partial x}\right)_{x=0} - \frac{\mu S_d}{kA}\frac{\partial P}{\partial t} = 0, \text{ for } t > 0 , \qquad (3)$$

$$P_u(t) = P_A \sin(\omega t + \delta) . \qquad (4)$$

In above equations, the coordinate x is chosen so that the downstream end of the sample is at $x = 0$. S_d is the storage of downstream reservoir. It is defined as volume V_d of fluid at pressure P, which must be injected/released from the reservoir in order to cause a unit change of pressure in that reservoir. Besides, the pressure P has been normalized to the initial pressure in the system so that $P(x, 0) = 0$. Eq. (2) shows that at the start of the experiment, the pressure inside the sample is uniform and is normalized to the initial mean pore pressure P_0. Eq. (3) is the mass conservation at the downstream face of sample. And Eq. (4) expresses the pressure oscillation at the upstream face of sample.

Detailed discussion on solving the above boundary problem can be found in Ref. [6]. Solutions are

$$P(x,t) = \alpha P_A \sin(\omega t + \delta + \theta) + 2P_A \omega k \mu A L^3 \beta_s^2$$

$$\times \sum_{m=1}^{\infty} \frac{\left[\cos(\psi_m x_D) - \dfrac{S_d \psi_m}{\beta_s AL}\sin(\psi_m x_D)\right]\psi_m^2 e^{-t_D \psi_m^2}}{(k^2\psi_m^4 + \mu^2\beta_s^2 L^4\omega^2)\left[(\psi_m^2 S_d - \beta_s AL)\cos\psi_m + (2S_d + \beta_s AL)\psi_m \sin\psi_m\right]} . \qquad (5)$$

Where, α is the amplitude attenuation, and θ is the phase shift, $t_D = \dfrac{k}{\mu\beta_s L^2}t$ and $x_D = \dfrac{x}{L}$ are normalized time and distance into the core, respectively, ψ_m satisfies the following equation:

$$\tan\psi_m = \frac{\beta_s AL}{S_d \psi_m} . \qquad (6)$$

Eq. (5) can be re-written as follows for simplicity,

$$P(x,t) = \alpha P_A \sin(\omega t + \delta + \theta) + \{\text{Transient Response}\} . \qquad (7)$$

It is clear from Eq.'s (5) and (7) that the pressure response along the sample includes two parts: a steady sinusoidal oscillation and a transient part with exponential decay. The steady response of the pressure along the sample will be a sinusoidal oscillation at the same frequency but with attenuated amplitude αP_A and a phase shift θ. Along the sample, α and θ has the following relation:

$$\alpha e^{i\theta} = \frac{(1+i)\sqrt{\dfrac{\xi}{\eta}}\cosh\left[(1+i)x_D\sqrt{\dfrac{\xi}{\eta}}\right] + i\dfrac{2AL\beta_s}{S_d\eta\xi}\sinh\left[(1+i)x_D\sqrt{\dfrac{\xi}{\eta}}\right]}{(1+i)\sqrt{\dfrac{\xi}{\eta}}\cosh\left[(1+i)\sqrt{\dfrac{\xi}{\eta}}\right] + i\dfrac{2AL\beta_s}{S_d\eta\xi}\sinh\left[(1+i)\sqrt{\dfrac{\xi}{\eta}}\right]} . \qquad (8)$$

In particular, at the downstream side of the sample,

$$\alpha e^{i\theta} = \frac{1}{\cosh\left[(1+i)\sqrt{\xi/\eta}\right] + \frac{1+i}{\sqrt{\xi\eta}}\sinh\left[(1+i)\sqrt{\xi/\eta}\right]}. \qquad (9)$$

Where η and ξ are defined as

$$\eta = \frac{2Ak}{\omega\mu LS_d}, \qquad (10)$$

$$\xi = \frac{AL\beta_s}{S_d}. \qquad (11)$$

In experiment, when the amplitude attenuation α and phase shift θ are measured, η and ξ can be solved from Eq. (9), thus both permeability and storage capacity can be calculated using Eq.'s (10) and (11).

EXPERIMENT
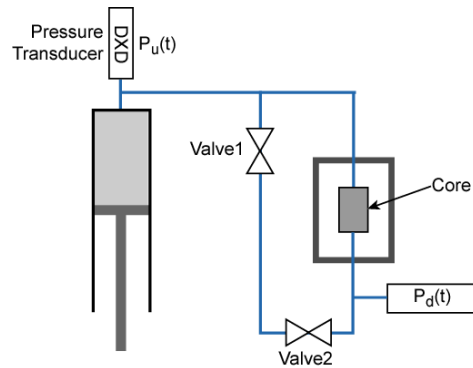
Figure 1: Schematic of sinusoidal pore pressure oscillation permeameter (SPPOP).

Measurements of gas permeability on tight samples have been performed in an apparatus called the sinusoidal pore pressure oscillation permeameter (SPPOP). The schematic of SPPOP is shown in Figure 1. The setup includes two computer controlled displacement pumps (only one is shown in the figure), a Hassler type core holder, pressure transducers and valves. For those two pumps, one is used to apply the confining stress, and the other one, as shown in Figure 1, is to apply pore pressure P_0 and generate pressure oscillation.

During a measurement, a dry, clean sample is first loaded into the core holder with a confining stress applied. It is then pressurized to certain pressure P_0 with nitrogen gas (N$_2$). After the pore pressure has been stabilized, a small pressure oscillation with its amplitude equal or less than 5 % of pore pressure is introduced at the upstream face. So $P_u(t) = P_A \sin(\omega t + \delta) + P_0$, and $P_A \leq 0.05 P_0$. Downstream pressure response $P_d(t)$ is measured. Nitrogen gas permeability (k_g) at that pore pressure can be calculated from the amplitude attenuation and phase shift of the downstream response using the above equations (9) – (11). The above procedure is repeated to measure gas permeabilities at four different pore pressures: 100, 200, 300, and 400 psig. An effective confining stress

of 1000 psi was applied on all other samples tested in this work, except for sample B1 where an effective stress of 850 psi was used. Gas Klinkenberg permeability was obtained from extrapolation of k_g vs. $1/P_0$ curve to where $1/P_0 = 0$ or $P_0 \rightarrow \infty$.

The samples we used in this work were from tight gas sand reservoirs and shale gas reservoir. They were typically 1 inch diameter and up to 1.5 inch length. They were cleaned and oven dried at 60 °C. The porosity ranges from about 3% to 12%. Table 1 lists parameters for those samples.

DATA ANALYSIS AND DISCUSSION
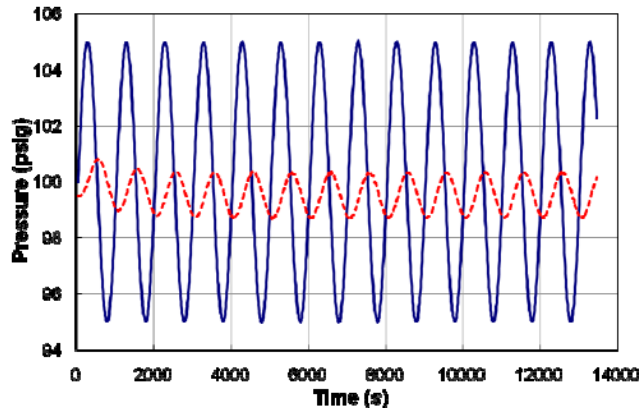
Figure 2: Upstream pressure oscillation with period $T = 1000$ s (solid line) and downstream response (dash line) of sample N1.
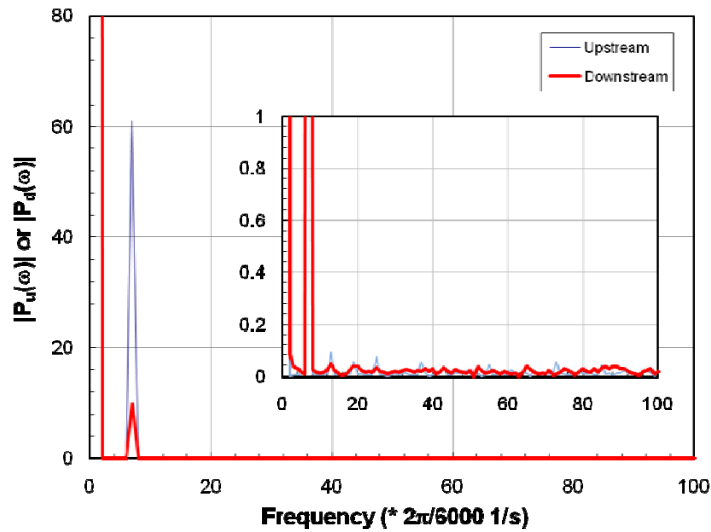
Figure 3: Amplitude spectrum of upstream (thin line) and downstream signal (thick line) for sample N1.

An example of measured raw data $P_u(t)$ and $P_d(t)$ on sample N1 is shown in Figure 2, where the oscillation period (T) was 1000 s, so the frequency was 0.001 Hz. The mean

pore pressure was 100 psig, and the upstream oscillation amplitude was 5 psi. The pressure oscillation amplitude was much smaller than the pore pressure. Therefore, the mean pore pressure along the sample remained constant. It is one of the advantages using pore pressure oscillation method as compared to the SS method, where a larger pressure drop has to be applied on the sample of inch long to measure certain flow rate. It eliminates the unwanted variation in both pore pressure and effective confining stress.

Fourier Analysis

Amplitude attenuation of downstream signal, α, was obtained from the amplitude spectrum of $P_u(t)$ and $P_d(t)$, and the phase shift θ was obtained through their cross spectrum. Fast Fourier Transform (FFT) has been used for the above Fourier analysis. Figure 3 shows the amplitude spectrum of the temporal data in Figure 2. In the figure, the strong DC components in both upstream and downstream signals were from the mean pore pressure P_0. Two peaks overlap each other at $\omega = 2\pi/1000 = 0.0063\,\mathrm{s}^{-1}$ represented the upstream driving signal and downstream response, respectively. The insert in Figure 3 is the same plot with vertical axis zoomed in to show that the downstream response at ω was well separated from other frequency components, such as room temperature fluctuation at very low frequency, noise from pump and pressure transducers, and other electrical noise at medium to high frequency. FFT in data analysis works as a filter. This filtering effect enhances the signal-to-noise ratio (SNR) and results in an increased sensitivity of measuring very low permeabilities. Those noises, on the other hand, exist in USS measurements and often complicate the data interpretation.

Transient Response
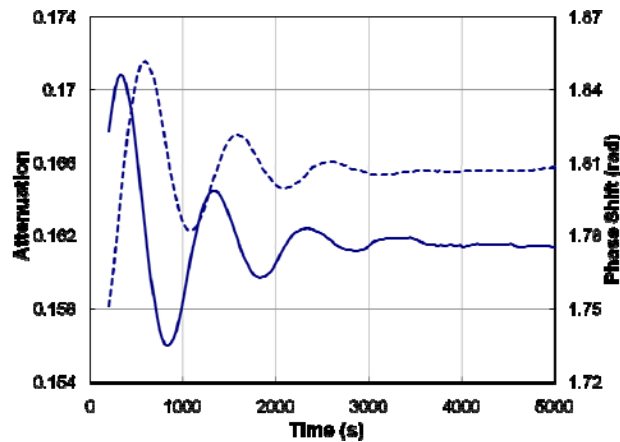
Figure 4: Amplitude attenuation α (solid line) and phase shift θ (dash line) of downstream signal as a function of time for sample N1.

From Eq.'s (5) and (7), the downstream pressure has a steady response and a transient part. The transient part decays exponentially with a time constant dependent on sample dimension, permeability, storage capacity, and fluid viscosity. In experiment, we typically record data for at least 8 cycles to ensure that the early time transient behaviour

has vanished. Figure 4 shows the downstream amplitude attenuation α and phase shift θ as functions of time for sample N1, where α and θ were obtained using FFT with a sliding time–window of 4 oscillation cycles long from raw data in Figure 2. It is seen from the figure that the steady response was indeed achieved after about 3 cycles of oscillation.

Frequency Dependence
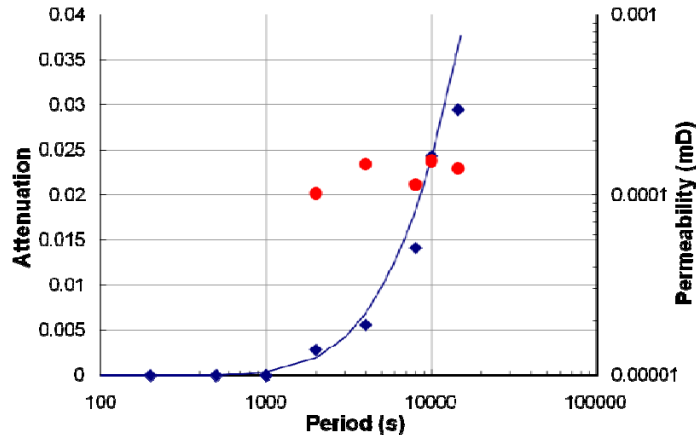
Figure 5: Relation between oscillation period and downstream amplitude attenuation (diamonds: experiment data; line: analytical calculation) and permeability (dots).
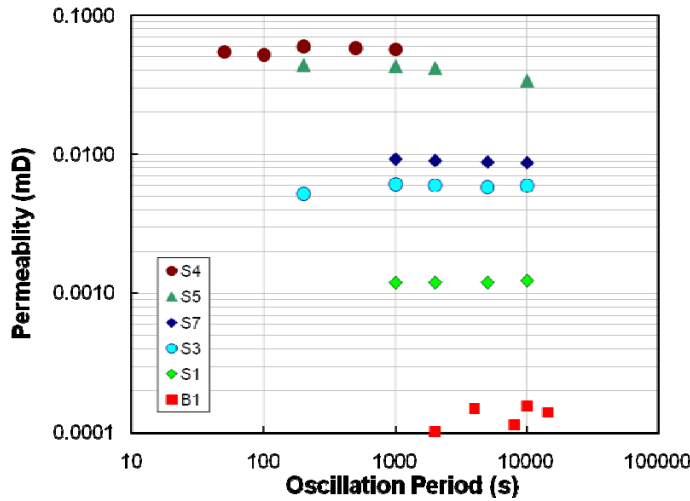
Figure 6: Relation between measured gas permeability and oscillation period for various samples.

Fluid flow in a porous medium described by Eq. (1) is a diffusion–like process, with a diffusivity of $k/(\mu\beta_s)$. On the other hand, in a pore pressure oscillation measurement, the gas flow in the sample changes direction at a frequency of ω. In experiment, this frequency has to be carefully chosen so that the gas flow can reach the downstream end of the sample, and cause downstream pressure increasing to a detectable level before flowing backward. By comparing diffusivity with oscillation frequency, it is suggested

that the lower the sample permeability, the longer the oscillation period should be. Figure 5 shows both the measured and calculated downstream signal attenuation as a function of oscillation period on sample B1, where Eq. (8) was used for the analytical calculation. Measured signal attenuation agreed well with that from analytical calculation. For this particular sample, if we need $\alpha > 0.01$, $T < 5000$ s would be useless, and $T = 10000$ s would be sufficient. On the other hand, as long as gas flow reaches the downstream side and certain signal-to-noise ratio (SNR) is reached; permeability can be deduced using this method. Gas permeabilities at a pore pressure of 100 psig with different oscillation period for sample B1are also shown in Figure 5. More measurements on different samples are shown in Figure 6. From both figures, the permeability does not depend on the frequency.

Method Comparison and Error Analysis
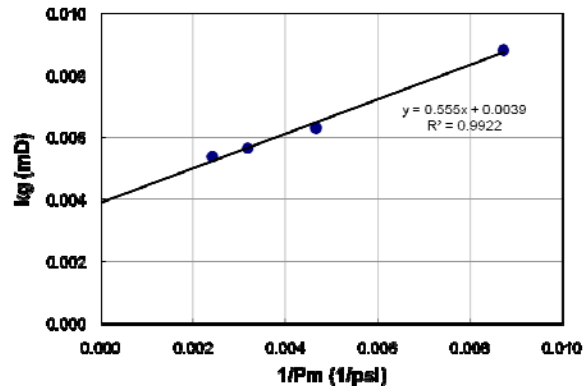
Figure 7: Klinkenberg permeability for a tight gas sample N1.

For all samples measured by SPPOP, Klinkenberg permeabilities were obtained to correct for the pore pressure dependence. Figure 7 shows an example for sample N1 with a Klinkenberg permeability of 0.004 mD. To calibrate the results from SPPOP, Klinkenberg permeabilities of S, J and N samples were also measured by SS method, which was made in the same Hassler type core holder with the atmospheric back pressure. The flow rate in SS method was measured by a mass flow meter or a bubble tube burette. Gas permeability was measured under four different delta pressures, i.e. 5, 10, 20 and 40 psi. Figure 8 shows the Klinkenberg permeabilities from both SS method and SPPOP. From the figure, in the range of 10^{-4} to 10^{-2} mD where the comparison has been made, permeability measured from SPPOP agrees well with that from SS method. More comparative measurements are needed and currently ongoing at the low permeability side ($<10^{-4}$ mD).

In Figure 8, error bars have been included for two samples S2 and S4, respectively. Errors in SPPOP measurements were estimated based on results with different oscillation frequencies. They mainly came from errors when solving nonlinear equation (9). Below we will discuss the associated uncertainties. Firstly, in our experimental setting, permeability can be measured more accurately than sample storage capacity. From Eq.'s (10) and (11), k and β_s have linear relation with η and ξ, which are related to α and θ

through a highly nonlinear equation (9). Therefore impact on k and β_s due to variations in α and θ are the same as that on η and ξ. Figure 9 (a) and (b) show the corresponding relative errors in k and β_s for certain change in α and θ, respectively. k varies linearly with respect to α and θ, i.e. 15% change in α or θ causes $\sim$ 20% change in k. On the other hand, β_s is greatly impacted by errors in α and θ. In particular, β_s can be up to 2.4 times higher given 15% error in θ.
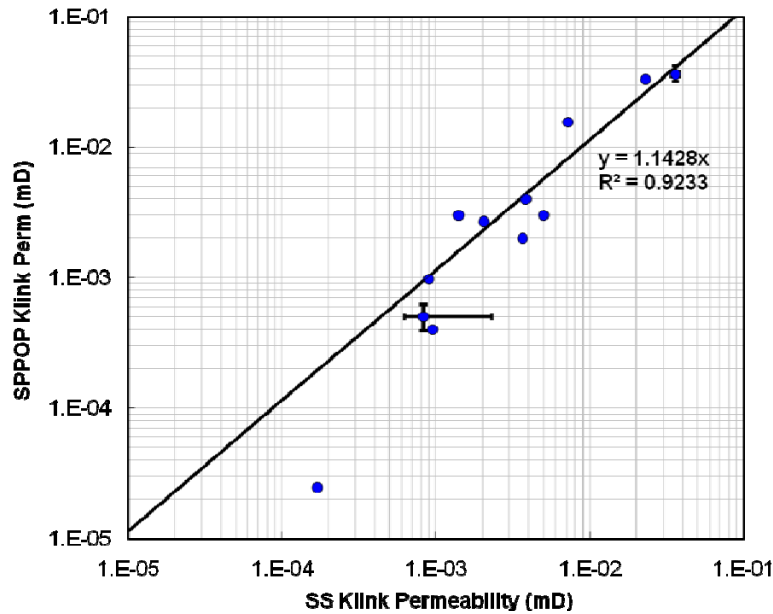
Figure 8: Klinkenberg permeability comparison on a set of tight gas samples between SPPOP and SS methods. Error bars are included for two samples to illustrate the uncertainties from both methods. See text for explanation.

Secondly, in a SPPOP measurement, both experiment itself and data analysis can introduce uncertainties in k (through α and θ). However, with proper system design and experimental parameter, most of those uncertainties can be greatly reduced. In data processing, the resolution in frequency domain is proportional to $1/\Delta T_0$, where ΔT_0 is the total length of data to be analyzed. In experiments, we typically record at least 8 cycles to ensure the steady response and better resolution in Fourier analysis. On the other hand, among those causing experimental errors, downstream storage (S_d) and oscillation period (T) are two most important parameters as they have great impact on α. Decreasing S_d through decreasing the volume of downstream reservoir, and increasing T will lead to larger α, thus improve the measurement resolution. In experiment, volume of the downstream reservoir is minimized, and S_d has been calibrated at different pore pressures. For different samples, T is chosen so that $\alpha > 0.02$ and proper SNR is achieved in frequency domain. Other sources of experimental errors include noise from pressure transducers, room temperature variations, noise and distortion in pump movement. As discussed above, by recording data with enough cycles, FFT can effectively filter out

those noises in frequency domain. With the above mentioned calibration and precautions, main uncertainty in a SPPOP measurement comes from error solving nonlinear equation (9).

(a)   (b)
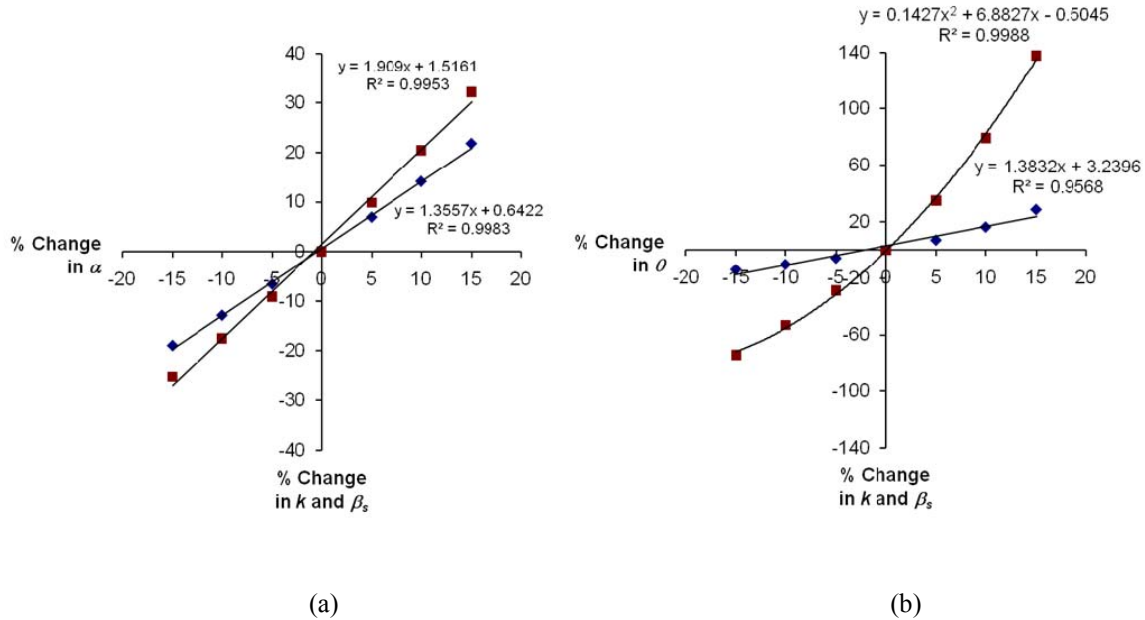
Figure 9: Relative change in k and β_s as results of a relative change in α (a) and θ (b), respectively.

In Figure 8, errors in SS measurements were mainly from the measured flow rate. For samples with relatively higher permeability ($\sim10^{-2}$ mD), uncertainties from both SPPOP and SS methods are both negligible. As the permeability decreases, uncertainty from the SS method increases greatly due to the difficulty in measuring small flow rate by mass flow meter. In contrast, error from SPPOP just increases slightly, and is much smaller. Therefore, SPPOP yields more accurate permeability characterization than that from SS method, especially in the micro and sub-micro darcy region.

Finally, as mentioned in the theoretical background section, we have solved a linear equation for gas flow analytically, with assumptions of small pressure change and constant compressibility. From the above discussion, during a pore pressure oscillation measurement, $P_A \leq 0.05P_0$, pressure drop across the sample is very small. For such small pressure variation, gas compressibility can be approximately considered as constant. Therefore, those assumptions are valid. Besides, the validity of a linear system assumption is also supported by the agreement between the measured frequency dependence of attenuation and that from analytical calculation (Figure 5), and by the agreement between SS Klinkenberg permeability and that from SPPOP. Research on more rigorous theoretical treatment is currently ongoing.

CONCLUSION

We have applied a pore pressure oscillation method in permeability characterization of tight samples from unconventional gas reservoirs. By introducing a very small pressure oscillation to the sample, we reduce the large pore pressure variation and are able to maintain pore pressure along the sample. Introducing FFT in data analysis enhances the signal-to-noise ratio, increases the sensitivity of measurement, and results in more accurate characterization. Moreover, pore pressure oscillation technique is non-destructive and can measure the permeability change continuously. It may find particular application in the study of permeability stress relation, in permeability assessment during core flood experiment, and in other physical or chemical process where permeability change plays a key role.

ACKNOWLEDGEMENTS

REFERENCES

1. Jones, S. C., "A Rapid Accurate Unsteady-State Klinkenberg Permeameter", *SPE Journal*, **12**, 383–397 (1972).
2. Hsieh, P. A., Tracy, J. V., Neuzil, C. E., Bredehoeft, J. D., and Silliman, S. E., "A Transient Laboratory Method for Determining the Hydraulic Properties of 'Tight' Rocks – I. Theory; II. Application", *Int. J. Rock Mech. Min. Sci. & Geomech. Abstr.*, **18**, 245-258 (1981).
3. Dicker, A. I. and Smits, R. M., "A Practical Approach for Determing Permeability From Laboratory Pressure-Pulse Decay Measurements", *SPE* 17578 (1988).
4. Egermann, P., Lenormand, R., Longeron, D., Zarcone, C., "A Fast and Direct Method of Permeability Measurement on Drill Cuttings", *SCA proceeding*, 2002-23, (2002).
5. Kranz, R. L., Saltzman, J. S., and Blacic, J. D. "Hydraulic diffusivity measurements on laboratory samples using an oscillating pore pressure method", *Int. J. Rock Mech. Min. Sci. Geomech. Abstr.*, **27**, 345-352 (1990).
6. Fischer, G. J., "The Determination of Permeability and Storage Capacity: Pore Pressure Oscillation Method", in *Fault mechanics and transport properties of rocks*, Evans, B. and Wong, T-f (Editors), New York: Academic Press, 187-211 (1992).
7. Bernabé, Y., Mok, U. and Evans, B., "A note on the oscillating flow method for measuring rock permeability", *Int. J. Rock Mech. Mining Sci.* **43**, 311 - 316 (2005).
8. Crawford, B. R., Faulkner, D. R., and Rutter, E. H., "Strength, porosity, and permeability development during hydrostatic and shear loading of synthetic quartz-clay fault gouge", *J. Geophy. Res. B: Solid Earth*, **113**, B03207, 2008.

9. Heller, K., Bruining, J., and Smeulders, D., "Permeability obtained from pressure oscillation experiments, Part I, one phase flow", in *Proc. XIVth international conference on computational methods in water resources, developments in water sciences*, Hassanizadeh, S. M., Schotting, R. J., Gary, W. G., and Pinder G. F. (Editors), Amsterdam: Elsevier, 201-207 (2002).

10. Boitnott, G. N., "Use of Complex Pore Pressure Transients to Measure Permeability of Rocks", *SPE* 38717 (1997).

Table 1: Core Dimensions and Properties

Sample #	Length (cm)	Diameter (cm)	Porosity (%)	k_ss (mD)	k_sppop (mD)
S1	3.918	2.530	5.9	9.5×10^{-4}	4.0×10^{-4}
S2	2.647	2.530	4.6	8.3×10^{-4}	5.0×10^{-4}
S3	3.360	2.533	5.9	1.4×10^{-3}	3.0×10^{-3}
S4	3.198	2.531	9.2	3.6×10^{-2}	3.6×10^{-2}
S5	3.830	2.532	8.7	2.3×10^{-2}	3.3×10^{-2}
S6	3.853	2.530	7.9	5.0×10^{-3}	3.0×10^{-3}
S7	3.861	2.526	8.9	3.8×10^{-3}	4.0×10^{-3}
S8	1.894	2.591	5.7	3.7×10^{-3}	2.0×10^{-3}
J1	2.695	2.528	8.7	7.2×10^{-3}	1.6×10^{-2}
J2	3.837	2.516	6.1	9.0×10^{-4}	9.7×10^{-4}
J3	2.495	2.531	4.4	1.7×10^{-4}	2.5×10^{-5}
J4	3.222	2.534	8.6	2.1×10^{-3}	2.7×10^{-3}
N1	3.169	2.539	11.8	1.9×10^{-3}	3.9×10^{-3}
B1	3.943	2.535	\	\	1.0×10^{-4}